New multispectral MRI methods may improve the diagnosis and tracking of Parkinson's disease

David A. Ziegler[1,2] Julien S. Wonderlick[1,2] Alex J. Murphy[1,2] John H. Growdon[3] Suzanne Corkin[1,2]

[1]Department of Brain & Cognitive Sciences, MIT, Cambridge, MA

[2]Athinoula A Martinos Imaging Center at the McGovern Institute, MIT, Cambridge, MA [3]Department of Neurology, MGH, Harvard Medical School, Boston, MA

Background

- Parkinson's disease (PD) is an age-related neurodegenerative disease that is characterized by progressive loss of dopaminergic neurons in the substantia nigra.[1]
- MRI is not currently used to diagnose and track PD because conventional methods lack sufficient sensitivity to visualize affected brain structures[2]

  For example, the substantia nigra is not readily apparent on conventional T1-weighted images:

histological section[3] | conventional MRI

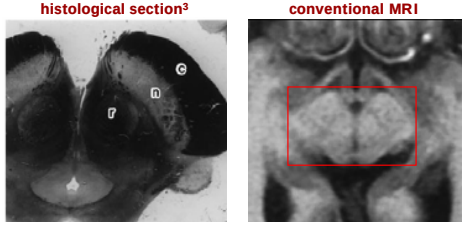

- Previous studies have imaged the substantia nigra using T2 relaxation times,[4] inversion-recovery sequences,[5,6] proton transverse relaxation rates,[6] and proton density weighted imaging.[3]
- A limitation of previous methods is that they were optimized to resolve a particular structure and are not ideal for visualizing other areas.
- We developed new MRI-based tools that use multispectral sequences to increase contrast, allowing visualization and morphometric characterization of midbrain structures implicated in PD pathology.

Methods

Participants

Group	*N*	Age*	Edu*	MMSE*
PD†	19	63.5 ± *7.4*	16.8 ± *1.8*	28.0 ± *1.8*
	9F/10M	(51–75)	(14–24)	(24–30)
CON	20	64.2 ± *7.2*	17.7 ± *2.6*	28.5 ± *1.7*
	11F/9M	(51–75)	(14–21)	(24–30)

* Scores are mean ± *SD* (range)

†Hoehn & Yahr stages: 0 (n=1), I (n=10), II (n=7), III (n=1)

†Unified Parkinson's Disease Rating Scale (UPDRS), motor subsection: *N* = 17, mean = 14.5 , range = 1-31

(UPDRS administered by neurologists at the MGH Movement Disorders Unit)

†Side of motor symptom onset: 17 right, 2 left

Image acquisitions

- Images were collected on a Siemens 3T Trio MRI system using a 12-channel matrix head coil
- We acquired bandwidth-matched multiecho T1, multiecho proton density, 3D T2-SPACE, and 3D T2-FLAIR sequences from each participant
- For each sequence, we collected a 3D slab consisting of 176 sagittal slices, 1.0 mm thick. In-plane field of view was 256 mm sampled on a 256 x 256 matrix, giving an in-plane resolution of 1.0 x 1.0 mm
  - Proton density weighting: we collected 6 echoes after a non-selective excitation with flip angle=3˚ and repetition time (TR)=20 ms
  - T1-weighting: we collected 4 echoes after a non-selective excitation with flip angle=7˚, TR=2530 ms, and inversion time (TI)=1100 ms
  - T2-SPACE: TR=3200 ms, TE=444 ms
  - T2-FLAIR: TR=6000 ms, TE=494 ms, TI=2100 ms
- All sequences were bandwidth matched at 698 Hz/pixel, minimizing the need for distortion corrections during coregistration

Multispectral image analysis

Individual multispectral images

multiecho T1 | T2-SPACE

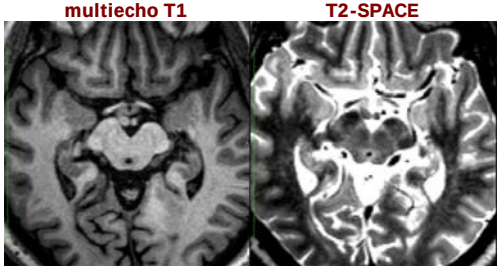

proton density | T2-FLAIR

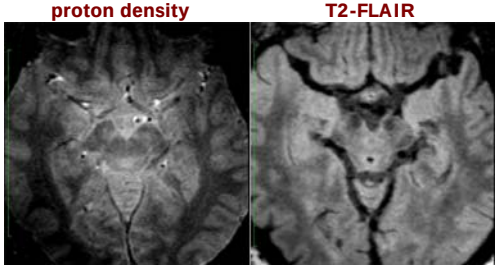

Multispectral weighted average

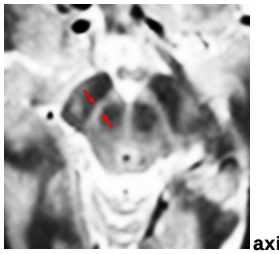

axial

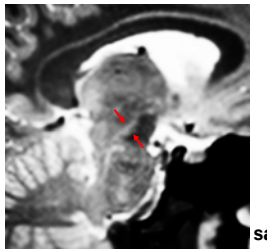

sagittal

- We used FreeSurfer and associated MNI tools for image analysis
- For each participant, we performed motion correction and averaging of multiple acquisitions separately for each multispectral sequence
- Next, we coregistered the four averaged, motion-corrected multispectral volumes for each participant using a linear rigid-body transformation with trilinear interpolation
- We then created a weighted average of the multiple echoes, yielding a single volume with a high contrast-to-noise ratio for the substantia nigra (red arrows)

Decreased signal intensity in the substantia nigra in PD

young adult (21,F) | older adult (69,F) | Stage II PD (69,F)

sagittal

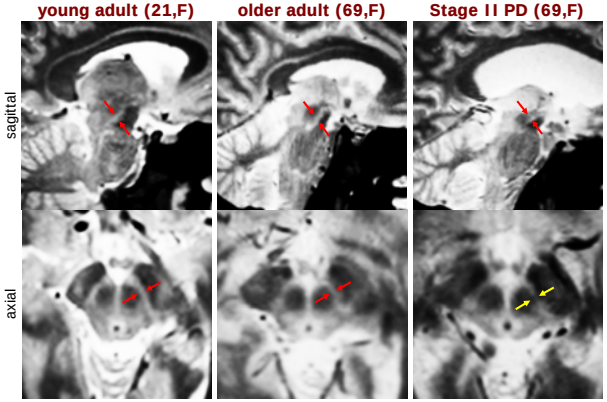

axial

- Multispectral weighted averages from three matched participants showing the substantia nigra (red arrows)
- The substantia nigra of the PD patient shows decreased signal intensity (yellow arrows); similar results were seen in 7 other patients
- The greatest signal loss occurred contralateral to side of motor symptom onset

Longitudinal data

- For 3 PD patients, follow-up scanning sessions were performed approximately two years after the initial visit with identical scanning parameters and equipment
- Comparison of the two scanning sessions showed subtle, but detectable, differences in signal intensity

Initial scan session

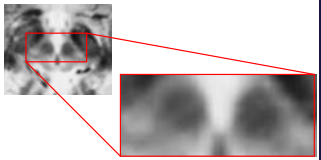

Follow-up scan session

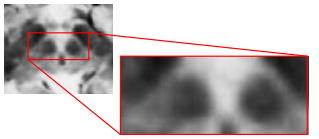

Nigral hyperintensities in PD patients

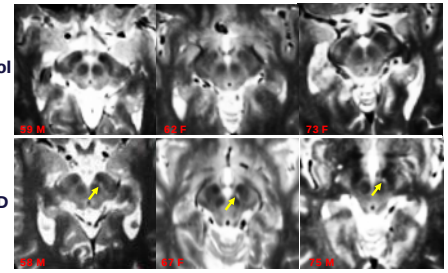

- A subset of PD patients (approximately 20%) exhibited hyperintense puncta in the substantia nigra, whereas none of the control participants showed these hyperintensities
- These hyperintense signals were contralateral to the side of motor symptom onset
- This signal change could be a viable marker for a subgroup of PD patients

Summary and future directions

- Here we describe a new method for combining multispectral MRI data to visualize the substantia nigra. Our preliminary analyses suggest that these multispectral methods will prove beneficial in the diagnosis and tracking of disease progression in PD patients.
- Inspection of multispectral weighted averages revealed a lateral to medial pattern of decreased signal intensity in the substantia nigra that was contralateral to the side of motor symptom onset in PD.
- We are developing an automated segmentation tool to label the substantia nigra, red nuclei, and cerebral peduncles; this tool will augment the FreeSurfer automated segmentation stream.
- We also discovered a subset of PD patients that displayed hyperintense puncta in the substantia nigra, possibly reflecting an abnormality arising from a distinct pathological process.
- Similar changes have been noted in T2-weighted images of Parkinsonian monkeys after exposure to MPTP,[8] and in a patient with St. Louis encephalitis.[9] Our observations appear to be the first report in idiopathic PD.

References

1. Fearnley & Lees (1991). *Brain, 114*: 2283-301.
2. Schrag et al. (1998). *J Neurol Neurosurg Psychiatry, 65*: 65-71.
3. Oikawa et al. (2002). *AJNR, 23*: 1747-56.
4. Kosta et al. (2006). *J Neurol, 253*: 26-32.
5. Hutchinson & Raff. (2000). *AJNR, 21*: 697-701.
6. Minati et al. (2007). *AJNR, 28*: 309-313.
7. Martin, Wieler & Gee. (2008). *Neurology, 70*: 1411-1417.
8. Miletich et al. (1994). *Ann Neurol, 35*: 689-697.
9. Cerna et al. (1999). *AJNR, 20*: 1281-1283.

Acknowledgements

• We thank Thomas Kemper and John Hedreen for assistance in delineating anatomical boundaries.
• This research was supported by NIH grants AG021525, DA022759-03, GM0007484, K23-AG22509 & T32 GM007484.
• The Athinoula A. Martinos Imaging Center at the McGovern Institute is supported in part by a generous gift from Pat and Lore McGovern.

Author contact information:

David Ziegler
daz@mit.edu
MIT 46-5125, 77 Mass. Ave
Cambridge MA 02139, USA